Structural Comparison between Oxidized and Reduced *Escherichia coli* Thioredoxin. Proton NMR and CD Studies†

Toshifumi Hiraoki, Simone B. Brown, Kenneth J. Stevenson, and Hans J. Vogel*
Division of Biochemistry, Department of Biological Sciences, University of Calgary, Calgary, Alberta, Canada T2N 1N4
Received June 17, 1987; Revised Manuscript Received March 11, 1988

ABSTRACT: *Escherichia coli* thioredoxin (M_r 11 700) usually functions as a hydrogen carrier protein that undergoes reversible oxidation/reduction reactions of its active-site disulfide linkage. By use of a number of assigned and identified resonances in one- and two-dimensional ^{1}H NMR spectra, the two forms of the protein have been compared. Only groups that are relatively close to the active-site Cys-32, Cys-35 linkage such as Trp-28, Trp-31, Phe-27, Ala-29, and Val-25 undergo substantial changes in their ^{1}H NMR chemical shift upon reduction. Various residues that are further removed from the active site, like Tyr-49, Tyr-70, His-6, Phe-12, Phe-81, and Phe-102, appear to be little affected (<0.02 ppm) by the reduction, suggesting that the rest of the protein structure is not much affected. Thus, the structural changes that occur upon reduction appear to be localized to the disulfide-containing turn and the central strand of the twisted β-sheet that directly leads to this turn. Notwithstanding the apparent similarity in the secondary and tertiary structures of the oxidized and reduced forms of the protein, the thermal stability of the protein decreases by 10 °C upon the reduction of the single disulfide. This was found by both ^{1}H NMR and near- and far-ultraviolet circular dichroism studies. Oxidized thioredoxin was also more resistant to alkaline denaturation. Furthermore, the exchange rate of the relatively stable slow-exchanging backbone amide protons that are part of the core of the twisted five-stranded β-sheet of thioredoxin increases substantially after reduction. These findings are discussed with reference to the reported effects of disulfides on the thermal stability of proteins.

Thioredoxin is a small ubiquitous protein that is intimately involved in a variety of redox reactions, such as the biosynthesis of deoxyribonucleotides (Laurent et al., 1964) and the reduction of inorganic sulfate and methionine sulfoxide (Black et al., 1960; Wilson et al., 1961) in microorganisms. It plays an important regulatory role in photosynthetic events (Wolosiuk & Buchanan, 1977), and its has also been implicated in the protein–disulfide exchange reactions that give rise to the proper folding of proteins that are stabilized by disulfide linkages (Holmgren, 1979; Pigiet & Schuster, 1986). In addition, it can participate as a structural rather than a reducing component in filamentous phage assembly (Russel & Model, 1986) and in T_7 viral DNA replication (Huber et al., 1986). The protein has been purified from a variety of sources (Holmgren, 1985), but the *Escherichia coli* protein, which is homologous with that from other sources, has been studied in the most detail. The amino acid sequence of its 108 residues has been determined both through amino acid sequencing (Holmgren, 1968) and by DNA-sequencing techniques (Lunn et al., 1984; Lim et al., 1985).

The crystal structure of the oxidized form of the protein ($TR\text{-}S_2$)[1] has been determined at 2.8-Å resolution (Holmgren et al., 1975), and a further refinement of this structure is presently underway (Eklund et al., 1984). $TR\text{-}S_2$ comprises an unusually high amount of secondary structure because it contains a single twisted β-pleated sheet composed of five strands that is surrounded by four α-helical segments. This overall folding pattern bears some resemblance to the NAD-binding domains that are found in many dehydrogenases (Holmgren et al., 1975). The active site of thioredoxin is made up of the two Cys-32 and Cys-35 residues that can be reversibly oxidized and reduced to form a cystine disulfide. This part of the protein forms a protrusion that is located between the center strand of the β-sheet and the second α-helix. So far, no protein crystals suitable for X-ray diffraction have been obtained for the reduced form of thioredoxin [$TR(SH)_2$] (Holmgren, 1985). This has prompted us to compare the structures of the oxidized and reduced forms of the *E. coli* protein by one- and two-dimensional high-resolution ^{1}H NMR studies. To date, only two preliminary one-dimensional proton NMR studies have been reported, and these have mainly concentrated on the detection of the resonances for the exchangeable NH protons (Holmgren & Roberts, 1976; LeMaster & Richards, 1985). The application of two-dimensional ^{1}H NMR techniques to the study of small proteins (M_r <20 000) has made it possible to determine a structure for a protein in solution (Wüthrich, 1986; Wemmer & Reid, 1985). Apart from total structural elucidations, the enhanced resolution in 2D NMR spectra compared to conventional 1D NMR spectra provides for a much more detailed "fingerprint" of a protein's conformation. Thus, 2D NMR spectra have been used to make comparisons between structures of independently folded domains and intact proteins (Drakenberg et al., 1987), oxidized and reduced forms of redox proteins (Moonen et al., 1984), and proteins with homologous amino acid sequences (Boyd et al., 1985). Here we have used a similar strategy to compare the structures for the oxidized and reduced forms of the thioredoxin.

† This project was sponsored by research grants from the Natural Sciences and Engineering Research Council of Canada (to K.J.S.) and the Medical Research Council of Canada (to H.J.V.). S.B.B. is the holder of a studentship and H.J.V. the recipient of a scholarship from the Alberta Heritage Foundation for Medical Research. This organization also provided the funds for the purchase of the NMR spectrometer.

[1] Abbreviations: NMR, nuclear magnetic resonance; CD, circular dichroism; TRS_2, oxidized thioredoxin; $TR(SH)_2$, reduced thioredoxin; COSY, two-dimensional *J*-correlated spectroscopy; nOe, nuclear Overhauser enhancement; NOESY, two-dimensional nOe spectroscopy; RELAY-COSY, two-dimensional relayed coherence transfer NMR spectroscopy; 2D, two dimensional.

0006-2960/88/0427-5000$01.50/0

Materials and Methods

Thioredoxin (TRS_2) was purified from the superproducing *E. coli* strain BH2012/$pCJF_4$ (Lim et al., 1985) as described earlier (Brown et al., 1987). This strain was kindly donated by Dr. J. A. Fuchs of the University of Minnesota. $TR(SH)_2$ was produced from TRS_2 by adding a 3–4-fold excess of dithiothreitol. NMR spectra were recorded on a Bruker AM-400 WB spectrometer that was equipped with a digital phase shifter and an ASPECT 3000 computer and array processor. Protein samples were dissolved in 0.1 M KCl and 99.8% D_2O or in 0.1 M KCl, 90% H_2O, and 10% D_2O. In all instances the field was locked onto the D_2O resonance. Deuteriated sodium 3-(trimethylsilyl)propionate-*2,2,3,3-d*$_4$ was used as an internal reference. The protein concentrations were 1–2 mM for all 1D NMR experiments and between 3 and 5 mM for all 2D NMR experiments. 2D NMR experiments were performed at 40 and 55 °C. A presaturation pulse for reduction of the HDO resonance was added where necessary, which was gated off during acquisition. The resolution in the 2D NMR spectra was enhanced by multiplication of the FID's with a nonshifted sine-bell function. The temperature calibration of the 5-mm ^1H NMR probe was carefully checked with a thermistor, and temperatures up to 75 °C were shown to be accurate to better than ±0.5 °C. D_2O (99.8%) was purchased from Merck, Sharp and Dome (Quebec, Canada) and dithiothreitol from Sigma (St. Louis, MO). All other chemicals used were of analytical grade.

All circular dichroism spectra were recorded on a Jasco J-500A spectropolarimeter equipped with a DP-500N data processor. The instrument was calibrated [with 0.1% *d*-10-camphorsulfonic acid (w/v in deionized water)] according to the procedure of Chen and Yang (1977). Protein solutions were placed in cylindrical cells with a path length of 1.0 mm for measurements in the far-UV region and 10.0 mm in the aromatic (near-UV) region. Temperature control of the sample cell was maintained by circulating water from a thermostatically controlled water bath through a built-in water jacket sleeve that is mounted around the CD cell. Temperature readings were measured online with a thermometer that was placed just before or after the cell. Cells were allowed a 5-min equilibration time upon reaching the desired operating temperature before scanning. Samples were typically scanned eight times from 250 to 205 nm, from 210 to 190 nm, or from 300 to 255 nm at 10 nm/min by using a time constant of 2 s and the automatic bandwidth selector. Spectra were electronically digitized, averaged, and smoothed before plotting.

The mean residue molar ellipticity ($[\Theta]_\lambda$) (deg cm^2 dmol^{-1}) at the given wavelengths of 280, 218, and 198 nm can be obtained by using the formula

$$[\Theta]_\lambda = \frac{(11700/108)\Theta_\lambda f}{100[P]l}$$

where l is the path length (cm), [P] is the protein concentration as determined by an A_{280} reading ($\epsilon = 13.6 \times 10^3$ M^{-1} cm^{-1}) (mol dm^{-3}), 11 700 is the molecular weight of thioredoxin containing 108 amino acids, and f is a scaling factor correcting the observed ellipticity Θ_λ in mm to mdeg [see Brown et al. (1987)].

Results

Assignments of the ^1H NMR Spectrum of Oxidized Thioredoxin. In the crystal structure the oxidized form of *E. coli* thoredoxin has a very well-defined and compact overall fold, as at least 75% of the residues are part of regular secondary structures (Holmgren, 1985). Figure 1 shows the ^1H NMR spectra of the oxidized form of *E. coli* thioredoxin dissolved in H_2O in D_2O for about 1 h. The presence of a well-defined fold is suggested by a series of ring-current upfield-shifted resonances for methyl groups between −0.6 and 1.0 ppm. In addition, the aromatic protons are well dispersed between 6.3 and 7.8 ppm. The resonances for the single Met and His residues can be easily assigned. The sharp singlet resonance for the ϵ-CH_3 of the single Met-37 residue appears close to 2.0 ppm. This assignment was confirmed by following its oxidation to the methionine sulfoxide by adding D_2O_2 or *N*-bromosuccinimide (data not shown). Both its chemical shift and its rate of oxidation indicate that its ϵ-CH_3 group faces the solvent. The resonances for the C_2 and C_4 protons of the single His-6 residue could be readily identified in Figure 1A and in a spin–echo spectrum (τ = 60 ms) in which four singlets were observed, two of which showed a pH-dependent behavior in the physiological pH range, thus confirming their assignment to His-6. The other singlet resonances are the two C_2 protons of the two Trp residues. A further noteworthy feature of the ^1H NMR spectra of Figure 1 is the presence of a series of resonances immediately downfield from HDO (4.6–5.8 ppm), with a total intensity of ~20 protons. Such resonances often form part of a β-sheet structure (Dalgarno et al., 1983; Pardi et al., 1983; Wüthrich, 1986). Furthermore, we found that irradiation of the resolved resonances between 5.0 and 5.8 ppm gave rise to nOe effects to other C_α protons in this spectral window, which is consistent with their being part of the β-structure. Indeed, in the crystal structure the β-sheet of thioredoxin contains about 22 hydrogen bonds (Holmgren et al., 1975). The presence of α-helices often reveals itself by giving rise to fairly intense nOe's between the backbone NH protons (Wüthrich, 1986). In a 2D NOESY spectrum we did indeed observe a few strong cross-peaks between NH protons, suggesting the presence of some α-helices (data not shown). Thus, these data are all in agreement with the presence of a β-sheet, α-helices, and an overall well-defined tertiary fold. The two most downfield resonances in the spectrum recorded in H_2O at 10.7 and 11.6 ppm belong to the two ring NH protons of Trp-31 and Trp-28, respectively (see below). These two protons, as well as the majority of all the backbone NH and all other exchangeable protons, have completely disappeared within 30 min when the protein is dissolved at 25 °C

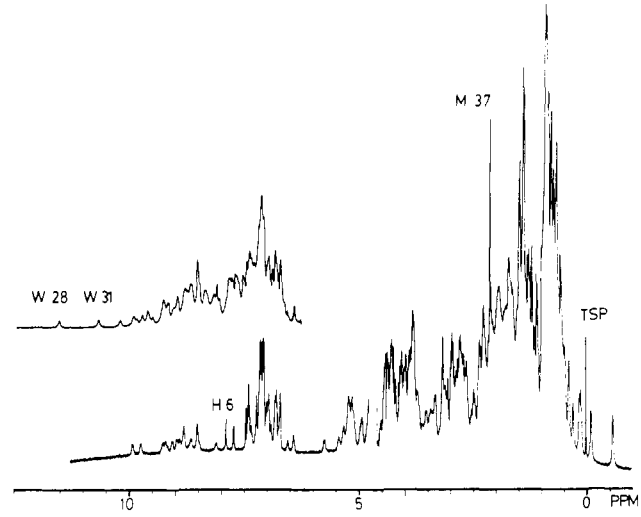

FIGURE 1: Proton NMR spectra of the oxidized form of *E. coli* dissolved in D_2O for 1 h (bottom) and in H_2O (top). The internal reference signal appears at 0 ppm, and the residual HDO resonance is at 4.62 ppm. The assignment of some resonances is indicated in the figure. The temperature was 55 °C, and the pH was 6.1. For further discussion see text.

Table I: Chemical Shifts of the Tentatively Assigned Resonances of *E. coli* Thioredoxin[a]

amino acid	protons	assignment
His	C_2 7.59; C_4 7.02	6
Phe-a	$C_{2,6}$ 6.82; $C_{3,5}$ 7.08; C_4 6.40; C_β 2.92/2.86; C_α 5.19	27
Phe-b	$C_{2,6}$ 7.17; $C_{3,5}$ 7.01; C_4 6.72; C_β 3.28/3.34; C_α 4.43	12/102
Phe-c	$C_{2,6}$ 7.05; $C_{3,5}$ 6.91; C_4 6.79; C_β 3.18/3.23; C_α 3.70	12/102
Phe-d	$C_{2,6}$ 7.43; $C_{3,5}$ 7.05; C_4 6.88; C_β 3.39/3.33; C_α 5.32	80
Tyr-a	$C_{2,6}$ 7.14; $C_{3,5}$ 6.70	70
Tyr-b	$C_{2,6}$ 7.13; $C_{3,5}$ 6.77	49
Trp-a	C_2 7.18; C_4 7.09; C_5 6.94; C_6 7.31; C_7 7.74; NH 10.7	31
Trp-b	C_2 7.46; C_4 7.40; C_5 7.20; C_6 7.15; C_7 7.41; NH 11.6	28
Ala	C_α 3.33; C_β 0.31	29
Val	C_α 3.77; C_β 0.77; C_γ −0.58/−0.28	25

[a] All values reported at 40 °C and pH 7.8, although some assignments in fact were made at 55 °C or pH 6.1.

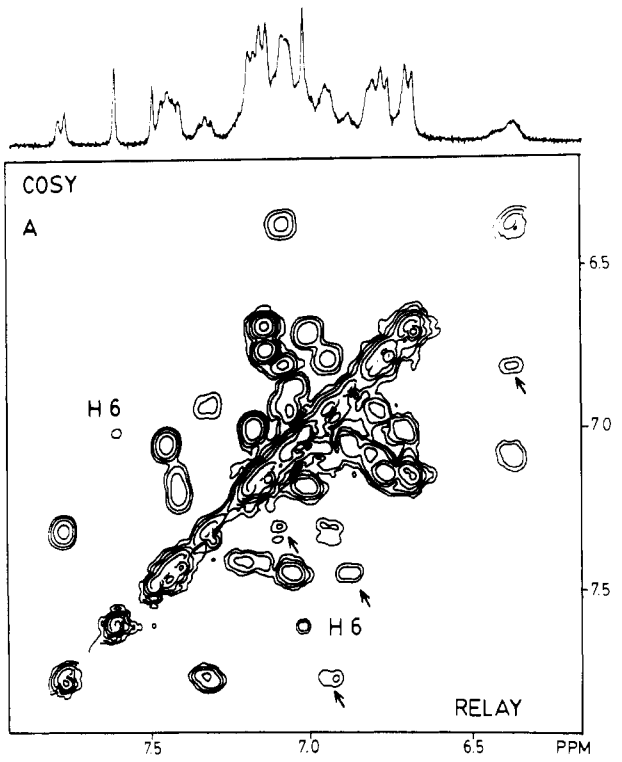

FIGURE 2: COSY and RELAY-COSY spectrum recorded at 40 °C, pH 7.8. Some of the extra relay peaks are indicated by the arrows, and the long-range cross-peaks for His-6 are labeled in both spectra.

in D_2O at pH 7.0. Approximately 15 backbone NH resonances between 8 and 10 ppm plus 1 amide proton (6.6 ppm) exchange much more slowly and are still present at almost full intensity after the protein has been dissolved for 1 h in D_2O.

E. coli thioredoxin contains a total of nine aromatic residues, one His, two Tyr, two Trp, and four Phe. The individual aromatic spin systems can be traced by following their through-the-bond connectivities in COSY and RELAY-COSY experiments recorded in D_2O (see Figure 2). In particular, the extra cross-peaks observed in the RELAY-COSY experiment greatly facilitated the identification of the cross-peaks belonging to individual Phe and Trp aromatic spin systems. In this fashion all the resonances could be readily identified. Even the long-range four-bond coupling between the His-6 C_2 and C_4 protons was observed in the COSY and RELAY-COSY spectra. The final step necessary for the completion of the total identification of all the aromatic protons is to connect the two Trp C_2 protons to their respective rings. This is most conveniently done by an nOe experiment in H_2O, making use of the fact that the ring NH is close to both the C_7 and the C_2 proton of a Trp (Boyd et al., 1985). Figure 3 shows the two relevant traces of a 2D NOESY spectrum that establishes the connectivities between the C_2 via the NH to

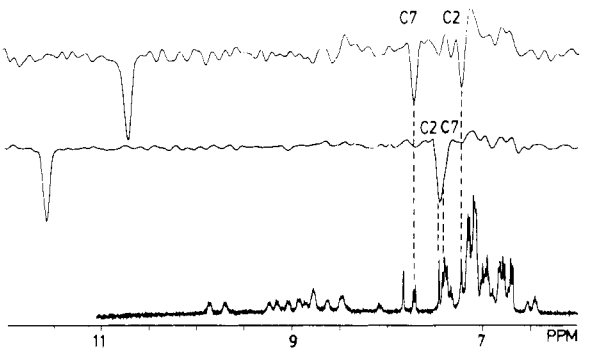

FIGURE 3: Traces from a phase-sensitive NOESY experiment in H_2O showing the proximity of the C_2 and C_7 resonances to the NH protons of the two Trp ring systems. The bottom spectrum shows a 1D NMR spectrum recorded in D_2O. All spectra were obtained at pH 6.2 and 55 °C. The assignment of the resonances is indicated in the figure. Because of the poor digital resolution (5 Hz/point) in the two traces, the C_2 and C_7 of Trp-28 are not resolved in the middle trace, but they are clearly separated in the bottom spectrum (0.5 Hz/point).

the C_7 protons. With this the identification of all the aromatic spin systems is complete, and they are listed in Table I. Also presented in the table are the chemical shifts for the aliphatic protons of the four Phe protons that could be readily distinguished in a NOESY spectrum recorded in D_2O (not shown).

In addition to the above, we performed a series of 1D nOe experiments (in D_2O) in which we irradiated all the clearly resolved resonances in the spectra. Irradiation (1.0 s) of the para proton of Phe-a gives a negative nOe effect to both the Trp-a C_5 and the two most upfield methyl resonances, which belong to one Val. Conversely, irradiation of the most upfield methyl protons (Val) results in a weak nOe effect to Trp-a C_5 and a strong one to the Phe-a ring protons. Irradiation of a peak at 0.31/0.29 ppm suggests spatial proximity of one Ala to Trp-a and Phe-a. With respect to the two tyrosines, we observed that the Tyr-a must also be relatively close to the Phe-a residue. Using the structure for the α-carbon backbone of the protein (Holmgren et al., 1975) that is available from the Brookhaven Protein Databank as a starting point, we introduced amino acid side chains using standard distances while following normal rules that apply to the folding of a protein. This molecular graphics model-building approach provides sufficient information to give tentative assignments of most of the resolved resonances in the ^1H NMR of *E. coli* thioredoxin. For example, Trp-28, Tyr-49, and Phe-102 all appear to be far removed from other aromatic residues. Thus, the nOe effects observed between Phe-a and Tyr-a are from Tyr-70, leaving Tyr-b as Tyr-49. The nOe effects between the Trp, Phe, Ala, and Val residues can only be due to Trp-31, Ala-29, Phe-27, and Val-25 because they are all on one side of the β-sheet, while Trp-28 is on the other side. Phe-d is also part of the β-sheet and is consequently assigned to Phe-80, leaving Phe-b and -c as Phe-12 or Phe-102, respectively.

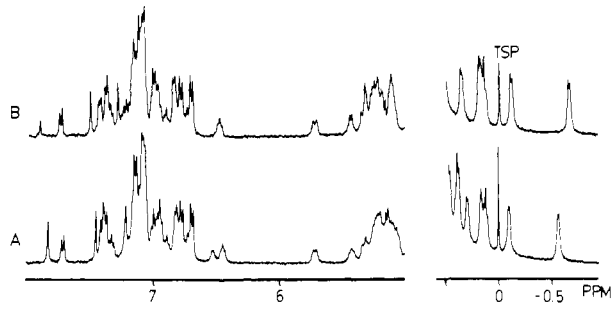

FIGURE 4: Comparison between the oxidized (A) and reduced (B) forms of thioredoxin. The spectra were recorded in D_2O at pH 6.1 and 50 °C. Backbone NH protons were not preexchanged, but those downfield from 8.5 ppm were not plotted. Only the region downfield from HDO and the upfield-shifted methyl region are shown.

Although a definitive and more complete assignment awaits the completion of the total sequence-specific assignment,[2] these data are sufficient to compare the oxidized and reduced forms of the protein.

Comparison of Oxidized and Reduced Thioredoxin by One- and Two-Dimensional NMR. The ^1H NMR spectra of oxidized and reduced thioredoxin at pH 6.1, 50 °C, recorded in D_2O are both plotted in Figure 4. Upon a first superficial inspection, the spectra for TRS_2 and $TR(SH)_2$ appear quite similar, suggesting that only small changes take place in the structure upon reduction. Moreover, the spectra for the NH protons, recorded for the protein dissolved in H_2O, are quite similar (data not shown). However, the most upfield shifted proton of Val-25 shifts further upfield by 0.12 ppm, whereas the singlet for the ϵ-CH_3 of Met-37 resonates at the same position (2.20 ppm, data not shown). The profiles for the C_α protons between 4.6 and 5.7 ppm and of some of the resolved backbone NH protons undergo some minor changes. It is also apparent that the aromatic NH proton for Trp-28 at 11.6 ppm experiences a larger change in chemical shift (0.2 ppm) than the one for Trp-31 (0.04 ppm), which resonates at 10.7 ppm [see also Holmgren and Roberts (1976)]. This is in agreement with comparative fluorescence studies of the *E. coli* and yeast thioredoxin which suggested that Trp-28 was more affected by the reduction than Trp-31 (Holmgren, 1972).

Figure 5 shows the pH dependencies recorded for the His-6 C_2 and C_4 protons and the resolved Trp-28 and Trp-31 C_2 and C_4 protons. The pK_a and Hill coefficients (Markley, 1975) as determined from these curves for His-6 in TRS_2 are $pK_a = 5.86 \pm 0.03$ and $n = 0.84 \pm 0.07$ and for $TR(SH)_2$ are $pK_a = 5.89 \pm 0.03$ and $n = 0.95 \pm 0.08$.[3] Thus, there appears to be no difference in the pK_a's of His-6. The value determined for the pK_a of His-6 is low compared to values of typical surface His residues that have a $pK_a \sim 6.8$ (Markley, 1975). The lower pK_a suggests that His-6, although exposed, interacts with another positively charged group, thereby decreasing its pK_a. Earlier fluorescence studies indicated that the steady-state Trp fluorescence was markedly influenced by a group with a pK_a of 6.5 (Holmgren, 1972; Reutimann et al., 1981). The lower pK_a of 5.8 determined for His-6 in this study indicates that it is an unlikely candidate for the foregoing group. This adds further support to the idea that the unusually low 6.7 pK_a of Cys-32 influences the steady-state Trp fluorescence (Kallis & Holmgren, 1980). Changes in the chemical shifts

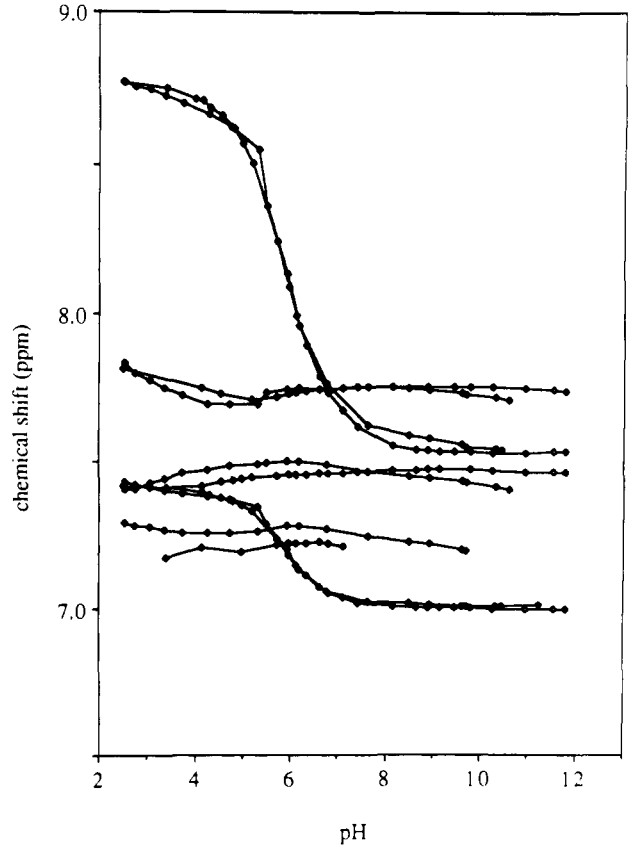

FIGURE 5: pH titration data for the C_2 and C_4 protons of His-6 (8.8 and 7.4 ppm at low pH), the C_2 proton of Trp-28 (7.25 ppm), and the C_4 and C_2 protons of Trp-31 (7.8 and 7.4 ppm at low pH). The open symbols are for TRS_2 and the closed symbols for $TR(SH)_2$.

of both Trp residues are apparent below pH 6 through to pH 2.5. These changes are probably caused by the aggregation of thioredoxin that occurs near its p*I* of 4.5 (Holmgren, 1985). Neither tyrosine residue experienced any changes in their chemical shifts when the pH was raised from 9 to 12 until the whole protein denatured (see below). Exposed tyrosine residues on proteins usually have pK_a values near 10.1 and exhibit a discernible pH titration behavior. Thus, we conclude that the phenolic hydroxyl groups of Tyr-49 and Tyr-70 are shielded from the solvent.

Because of the higher resolution in 2D NMR contour plots compared to that of 1D NMR spectra, it is possible to make a more detailed comparison of the two forms of *E. col* thioredoxin by studying the changes in the patterns of cross-peaks obtained in two-dimensional COSY-spectra (Moonen et al., 1984; Wüthrich, 1986). Such a comparison is made in Figures 6 and 7 for the aromatic protons and the Ala/Thr region of the COSY spectrum. The most prominent changes are indicated by the arrows. In Figure 6, it can be seen that Trp-28 (solid arrow) and Trp-31 and Phe-27 (dotted arrows) experience a change. The most marked changes are for Trp-28 (solid arrow). However, in contrast, the cross-peaks for the two Tyr resonances (49 and 70) and the other three Phe resonances (12, 81, and 102) remain at identical chemical shift positions. Similarly, in the Ala/Thr region, in Figure 7, we noted a large change for the Ala-29 resonance, which is indicated by the arrow. Also, two other cross-peaks, which have been identified as Ala but are not assigned at this stage, experience a small upfield shift (see dotted arrows). However, all 15 other Ala and Thr resonances are unaffected. Also, the cross-peaks between the methyl groups and their coupled protons in the Ile/Leu/Val part of the spectrum appear similar to those for TRS_2 and $TR(SH)_2$ (data not shown). Some small

[2] While this paper was under review, a sequential assignment for the NH, α, and β protons of *E. coli* thioredoxin was reported (Le Master & Richards, 1988).

[3] The reported values represent the averages recorded for the C_2 and C_4 protons.

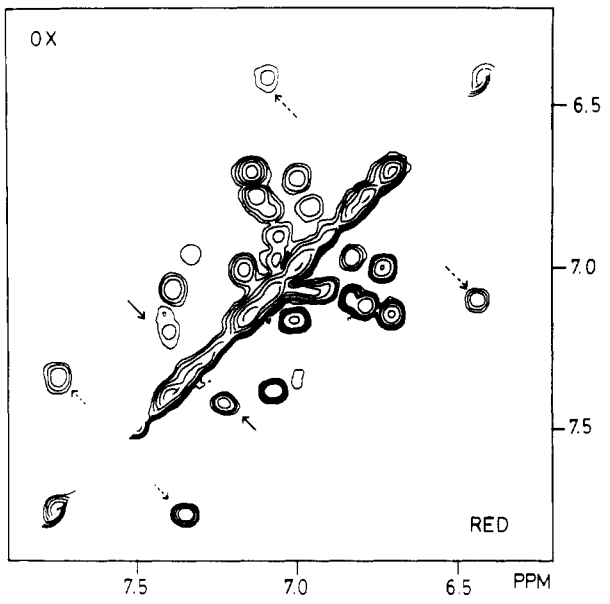

FIGURE 6: Combined contour plots for the two-dimensional COSY (RED) and double-quantum-filtered COSY (OX) experiments for the oxidized (OX) and reduced (RED) forms of *E. coli* thioredoxin recorded at pH 7.8. The solid arrow indicates the major change for Trp-28, and the dotted arrows indicate a change for Trp-31 and Phe-27.

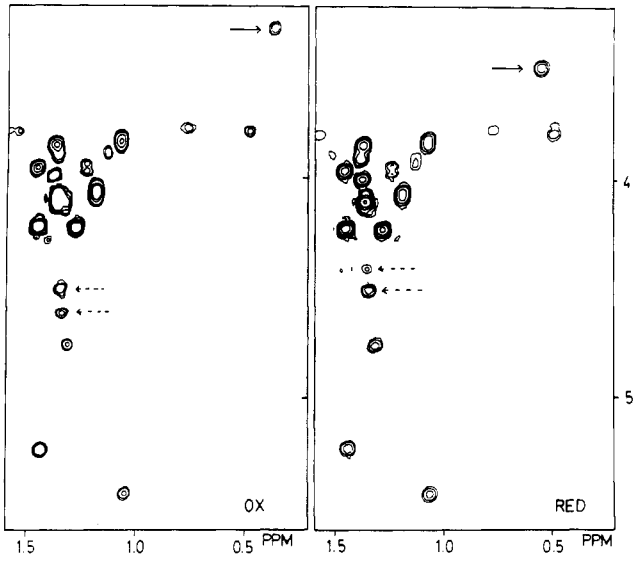

FIGURE 7: Parts of the COSY spectra for oxidized (OX) and reduced (RED) forms of thioredoxin showing the area containing the Ala and Thr cross-peaks (pH 7.8). For further discussion see text.

changes occur for some of the resonances, such as Val-25, but the changes are all within 0.15 ppm, suggesting relatively minor adjustments of the structure. In this respect it is noteworthy that a change of 0.1 ppm for these methyl protons that are upfield shifted due to their proximity to aromatic rings corresponds to a change of only 0.01 nm in their distance to the ring or to a small rotation (Perkins, 1982).

Alkaline and Temperature Denaturation Studies. In the course of the pH titration experiments, performed at 25 °C and a 1 mM protein concentration, a significant amount of precipitation occurred between pH 3.5 and 5.5. Nevertheless, a 1D NMR spectrum was still visible, allowing us to record a complete pH profile. At pH 2.5 both TRS_2 and $TR(SH)_2$ are stable and no signs of any denaturation could be detected in the spectra. Close to the alkaline pH extreme we noted that TRS_2 was still fully stable at pH 11.5 but that new peaks for the denatured form started to appear above this value and that

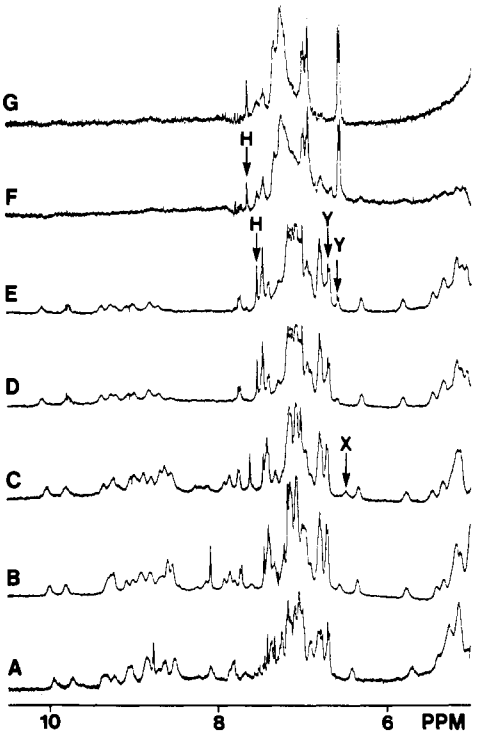

FIGURE 8: pH dependence of the spectra of TRS_2 showing the alkaline denaturation, which is in slow exchange on the NMR time scale (25 °C, 1 mM protein concentration): (A) pH 2.5; (B) pH 6.0; (C) pH 7.4; (D) pH 11.5; (E) 11.8; (F) pH 12.2; (G) pH 12.5. The arrows indicate the resonance for tyrosines (Y) and histidine-6 (H) and a slowly exchanging NH proton (X). The midpoint of the alkaline denaturation is at pH 12.0.

the alkaline denaturation was complete at pH 12.5 (see Figure 8). From the appearance of separate resonances for the native and denatured form of TRS_2, it is clear that these two forms are in slow exchange on the NMR time scale. From the chemical shift changes for the protons on the His-6 and Tyr residues, we could deduce that the exchange rate between the two forms was $\ll 300\ s^{-1}$. For $TR(SH)_2$ we noted that the midpoint for the alkaline denaturation was at pH ~ 11 and that the exchange rate also was $\ll 300\ s^{-1}$. Shifting the pH back to 7.0 allowed both the alkaline denatured TRS_2 and $TR(SH)_2$ to refold to a large extent to their native conformation, although the process was very slow and was still not complete after 24 h (data not shown). Inspection of Figure 8 also reveals that changes occur in the C_α protons downfield from the HDO resonance throughout the whole pH range. Nevertheless, they only shift to their random coil position upfield from HDO when the protein denatures. One final point of interest about the pH titrations was that the slow exchanging NH proton, which appears at 6.5 ppm in the spectrum of TRS_2, shifts to higher field at pH values around 9 and is no longer observable below pH 4.0 (see Figure 8).

Figure 9 shows the spectra of TRS_2 obtained at a series of temperatures. At temperatures above 60 °C all the exchangeable NH protons disappear. The midpoint of the denaturation of TRS_2 is at 80 ± 1 °C, and the transition appears to be cooperative as all unusually shifted resonances (aromatic, methyl, and C_α protons) shift simultaneously to their random coil positions. No evidence for slow reactions could be found as the spectra remained the same for up to 3 h at any given temperature. The exchange rate between the native and denatured forms is again slow on the NMR time scale ($\ll 300\ s^{-1}$). One other interesting feature that can be noted from Figure 9 is the strong temperature dependence of the chemical shifts of the Val-25 and Phe-27 resonances. Such behavior

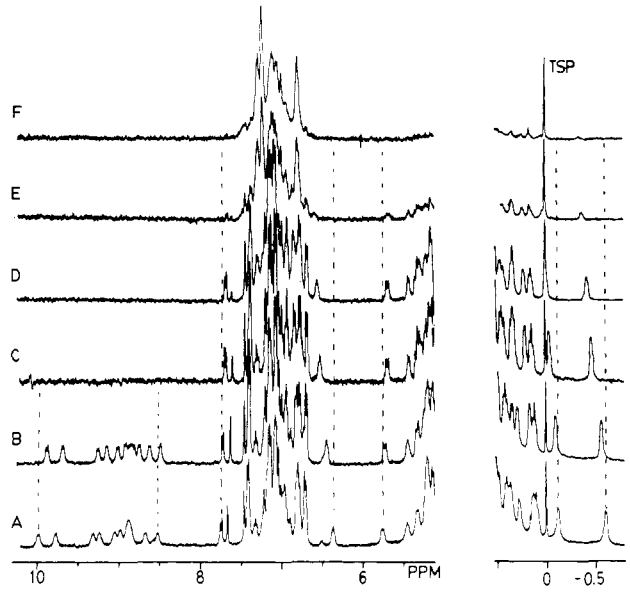

FIGURE 9: Temperature dependence of the ^1H NMR spectrum of oxidized thioredoxin. The temperatures were (A) 30 °C, (B) 50 °C, (C) 70 °C, (D) 75 °C, (E) 80 °C, and (F) 82 °C. For discussion see text.

is consistent with the notion that these shifts are mainly caused by ring-current effects. For $TR(SH)_2$ the midpoint of the denaturation was 71 ± 1 °C. The spectra were otherwise similar to those obtained for TRS_2 except that the denaturation gave rise to much broader spectra (data not shown), possibly as a result of a faster exchange rate between native and denatured forms or, alternatively, as the result of aggregation caused by intermolecular disulfide formation. The thermal denaturation of both TRS_2 and $TR(SH)_2$ was reversible to a large extent but again very slow (~24 h), as we had observed earlier for the alkaline denatured protein.

The denaturation of TRS_2 and $TR(SH)_2$ was further studied by circular dichroism performed at three different wavelengths that could provide some indications about the integrity of various structural elements. For the ellipticity in the far-UV region the Θ_λ^{218} is thought to contain contributions from all secondary structural elements, and Θ_λ^{198} contains proportionally a higher contribution from α-helices (Chen et al., 1974; Siegel et al., 1980). The ellipticity in the near-UV region (Θ_λ^{280}) is strongly dependent upon the asymmetric environment around the aromatic chromophores and is thus also sensitive to the overall folding of the protein. The data obtained for TRS_2 and $TR(SH)_2$ are shown in Figure 10. The mean transition temperature (T_m) for TRS_2 was determined at 89 ± 1 °C and at 78 ± 1 °C for $TR(SH)_2$ when the ellipticity at 218 nm was followed. However, when the transition was followed at 198 nm, $TR(SH)_2$ appears to denature with a T_m of 71 ± 1 °C, whereas the denaturation curve for the TRS_2 is no longer cooperative to the same extent and may even be biphasic, as shown in Figure 12A, with respective T_m's of 89 and 80 ± 1 °C. If the data at 218 nm for the denaturation of TRS_2 are interpreted as one rather broad transition, the denaturation temperature is 85 ± 1 °C. Figure 10C shows the thermal transitions obtained in the near-UV region. First, there is a gradual loss of ellipticity up to 50–70 °C, reflecting the increased thermal motion of the aromatic chromophores. The subsequent cooperative denaturation for TRS_2 occurs at 81 ± 1 °C and for $TR(SH)_2$ at 72 ± 1 °C.

Backbone Amide Proton Exchange. Wagner and Wüthrich (1979) have demonstrated that there is a correlation between the backbone amide proton exchange rates and the denaturation temperatures for a series of homologous small globular proteins. Thus, to complement our denaturation studies, we compared these exchange rates for the two different forms of thioredoxin. As we have shown in Figure 1, the majority of the NH protons exchange very rapidly at pH 7.1 as they cannot be detected in the ^1H NMR spectrum of freshly dissolved TRS_2 in D_2O. However, about 15 backbone NH resonances were readily detected, as they appeared to exchange slowly. Figure 11 shows two parts of the contour plot of a COSY spectrum that was recorded at 40 °C, pH 7.8, for a freshly dissolved protein in D_2O. Using the connectivities observed in Figure 11, we could identify a series of the slowly exchanging resonances to Ala, Ile, and Thr residues, as is indicated in the figure. Interestingly, the majority of the slowly exchanging NH protons are coupled to α-carbon protons that resonate between 5 and 6 ppm. Such a pattern is consistent with these protons being part of the β-sheet of TRS_2. Indeed, the β-sheet is mainly made up of hydrophobic residues, and it forms the core of the protein (Holmgren et al., 1975). Therefore, it would be expected to be the least exposed part of the protein.

Figure 12 shows the decrease in intensity for these β-sheet backbone hydrogens for both the TRS_2 and $TR(SH)_2$ as measured at 50 °C, pH 7.1. There are 2–3 resonances that disappear relatively fast. However, the remaining 11–12

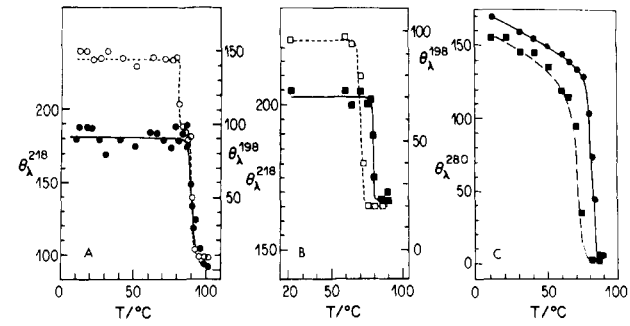

FIGURE 10: Thermal denaturation profiles determined by far-UV circular dichroism for oxidized (A) and reduced (B) thioredoxin recorded at wavelengths of 218 (closed symbols) and 198 nm (open symbols). Experimental conditions: (A) [P] = 22.8 μM, f = 0.075 mdeg/mm (218 nm) and 0.20 mdeg/mm (198 nm); (B) [P] = 11.8 μM, f = 0.04 mdeg/mm (218 nm) and 0.12 mdeg/mm (198 nm). The thermal denaturation profiles determined in the near-UV CD are shown in (C) for the oxidized and the reduced protein. Conditions: [P] = 26.8 μM and f = 0.025 mdeg/mm.

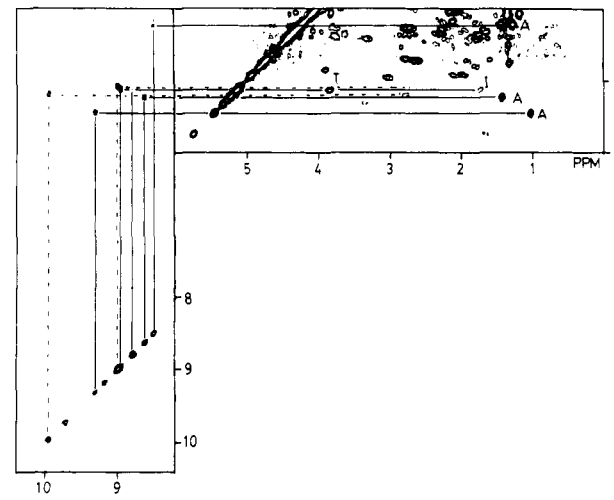

FIGURE 11: Two parts of a COSY spectrum recorded for a sample of oxidized thioredoxin that was freshly dissolved in 99.8% D_2O, pH 7.8. The connectivities and identifications of the resonances for the slowly exchanging NH protons are indicated in the figure.

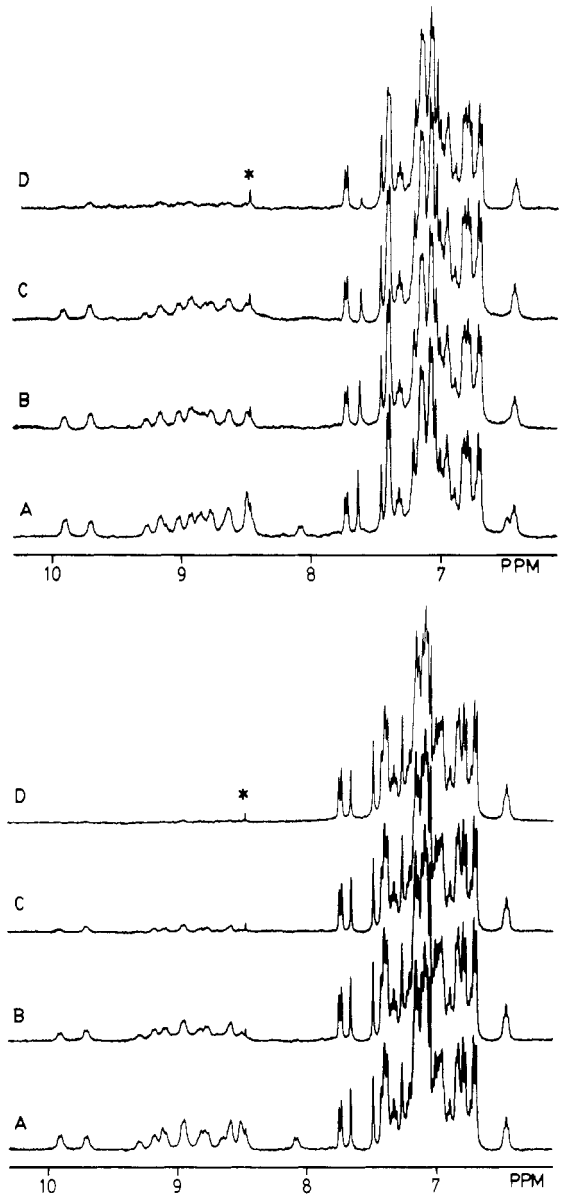

FIGURE 12: (Bottom) Exchange rates for slowly exchanging NH backbone protons of reduced thioredoxin at 50 °C and pH 7.1. The times at which the spectra were recorded were (A) 50 min, (B) 2.3 h, (C) 4.3 h, and (D) 10.3 h. The asterisk indicates a small amount of impurity. (Top) Exchange rates for the slowly exchanging NH–backbone 7.1. The times at which the spectra were recorded were (A) 10 min, (B) 10.8 h, (C) 32.8 h, and (D) 67.5 h.

residues all disappear at a rate that appears to be common to this entire group of exchangeable protons. The rate measured for the TRS_2 β-sheet hydrogen exchange is at least 10 times slower than that for $TR(SH)_2$ at 50 °C. Very little intensity remained for $TR(SH)_2$ after 4.3 h, whereas some intensity is still apparent for TRS_2 even after 67.5 h. From Figure 12 it can also be seen that the C_2 proton of His-6 (7.62 ppm) has exchanged almost completely with deuterium from the D_2O after 67 h at 50 °C. This again suggests that His-6 is in a position where it is accessible to solvent.

Discussion

The oxidized and reduced forms of thioredoxin have been studied extensively by various spectroscopic measurements, most notably by steady-state fluorescence and circular dichroism techniques (Stryer et al., 1967; Holmgren, 1972; Reutimann et al., 1981; Brown et al., 1987). The information that can be gathered by fluorescence about structural changes throughout the protein is somewhat limited as the Trp-28 and Trp-31 residues that dominate the fluorescence spectrum are both close to the disulfide active site. Nonetheless, the fluorescence spectrum does undergo substantial changes upon the reduction of the disulfide, which could reflect conformational changes in the vicinity of the active site (Stryer et al., 1967; Brown et al., 1987). However, Holmgren (1972) has pointed out that the cystine disulfide linkage should provide an efficient quencher of the Trp fluorescence. This raises some doubts about the extent, if any, of such a conformational change, as the change in fluorescence could simply be the removal of this quenching group. Deductions about secondary structural elements in proteins can normally be made quite reliably from CD studies (Chen et al., 1974; Siegel et al., 1981). The far-ultraviolet CD spectra for TRS_2 and $TR(SH)_2$ are reported to be quite similar (Stryer et al., 1967; Reutimann et al., 1981; Brown et al., 1987), which would suggest that the secondary structure of the two forms of the protein are closely related. However, there is very little agreement between the amount of secondary structure as calculated from the CD data and that observed in the crystal structure (Reutimann et al., 1981; Brown et al., 1987). In addition, the complex transitions observed in the CD temperature denaturation experiments (see below) provide a further indication that the relative contributions of various structural elements to the CD spectra are poorly understood for this protein at the present time.

The NMR data presented in this paper provide a more detailed insight into the structural changes that accompany the reduction of TRS_2. Fortuitously, the aromatic resonances, which have been identified and tentatively assigned, are strategically placed as spectral reporter groups throughout the protein. Thus, the comparative 1D and 2D NMR data suggest conclusively that the changes in the overall stucture upon reduction of thioredoxin in the pH range 2.5–10.5 remain limited to the turn encompassing the disulfide bridge (Trp-31) and to the β_2-strand (Val-25, Phe-27, Trp-28, Ala-29) that precedes this turn. Changes in the disulfide-containing loop have also been observed for small synthetic peptides that resemble the disulfide active site of thioredoxin (Kishore & Balaram, 1986). Unfortunately, our data about possible changes for the α_2-helix, which is attached at the C-terminal side of the disulfide turn, are somewhat less conclusive at this stage. Both the ϵ-CH_3 of Met-37 and the aromatic protons of Tyr-49, which is at the end of this helix, are unaffected. However, as neither residue appears to be close to any aromatic residues and as the Met-37 side chain points toward the solvent in both forms, one would not expect to detect large chemical shift changes for these two residues if the α_2-helix would move with respect to the β-sheet following the reduction as has been suggested (Brown et al., 1987). Notwithstanding the above, the aromatic residue that appears to be most affected by the reduction of TRS_2 to $TR(SH)_2$ is Trp-28, which may indicate some movement of part of the α_2-helix. The fact that none of the spectral reporter groups, which are further away from the active site, undergo any changes in chemical shift upon reduction is consistent with the idea that the remainder of the structure is very similar in both forms, if not the same.

The covalent cross-linking of protein chains through the formation of disulfide bonds provides an important means for the stabilization of proteins against thermal denaturation (Anfinsen & Scheraga, 1975). For example, the introduction of extra disulfide bonds through protein engineering techniques in dihydrofolate reductase (Villafranca et al., 1983), T_4 lysozyme (Perry & Wetzel, 1986), and the λ-repressor (Sauer et al., 1986) offers a considerable improvement in the pro-

Table II: Denaturation Temperatures Measured for Oxidized and Reduced Thioredoxin at pH 7.0[a]

technique	TRS_2	$TR(SH)_2$
NMR	80	71
CD (280 nm)	81	72
CD (218 nm)	89	81
CD (198 nm)	85	71
literature	85,[b,c] 82[d]	73[b]

[a] Values (±1 °C) as determined in this report. [b] Quoted by LeMaster and Richards (1985). The value for $TR(SH)_2$ was determined in calorimetric measurements. [c] Reutimann et al. (1981) reported, on the basis of CD data, that TRS_2 was stable in the range 2–80 °C. [d] Determined by Kelley et al. (1987).

tection of these proteins against thermal (ΔT_m 10–20 °C) or urea denaturation. In addition, the selective reduction of one disulfide linkage in the small bovine pancreatic trypsin inhibitor results in a substantial decrease ~30 °C) in its thermal stability (Wagner et al., 1979). On the basis of these data, the introduction of disulfide linkages may provide an important means for improving the thermal stability of biotechnologically relevant proteins. The disulfide linkage at the active site of thioredoxin is different from the ones in these other proteins because it does not cross-link different segments of the protein and only a small 14-membered disulfide loop is formed. It is difficult to envisage how this could confer a similar increase in the thermal stability of the protein. Because the same -Cys-X-Y-Cys- 14-membered disulfide ring appears at the
 └S—S┘
active site of a large number of redox proteins with disulfide active sites [cf. Holmgren (1985)], it is of general interest to determine the effect of this small loop on the overall thermal stability of the protein. The data obtained here demonstrate that the formation of the small disulfide loop does indeed stabilize the protein to a degree comparable with that for the other proteins. The reduction of the protein not only lowers the thermal stability of the protein by 10 °C (see Table II) but also decreases the midpoint for the alkaline denaturation by 1 pH unit. As discussed earlier, it is unlikely that other structural elements (α-helices, β-sheet) are changed much by the reduction, and thus the differences in the thermal stability are related to the presence or absence of the disulfide bond. The data in Table I deserve further comment. First, the T_m values determined by NMR are in close agreement with those obtained in the near-ultraviolet CD studies. Also, the T_m value obtained at Θ_{198} and reported T_m values were the same within experimental error as the NMR results. However, the CD data recorded at a wavelength of 218 nm suggest a considerably (~10 °C) higher stability for both TRS_2 and $TR(SH)_2$. Although these data are expected to be dependent on the concentrations of protein and salt, this would not be sufficient to explain the differences between the experiments. Thus, this may indicate that the different structural elements do not have exactly the same thermal stability and that partially unfolded structures may exist. It is not clear, however, why such intermediates do not reveal their presence in the NMR spectra recorded during the temperature denaturation (see Figure 9). Nevertheless, this interpretation is in keeping with the complex refolding behavior of TRS_2 and $TR(SH)_2$, which is known to take place in not less than three phases and is different for both forms of the protein (Wilson et al., 1986).

The analysis of backbone hydrogen-exchange data for individual sites in a protein can provide important information about the motional dynamics in different parts of proteins (Woodward et al., 1982; Wagner, 1983; Kosiakoff, 1982). The data presented in Figures 1, 11, and 12 are consistent with the idea that the central part of the β-sheet of thioredoxin exchanges its hydrogens slowly compared to the rest of the protein. It is of interest that the rates for the exchange of these β-sheet protons are equal within the error of the determinations. Furthermore, the exchange rate increases substantially upon the reduction of the protein. Such behavior was expected on the basis of differences in denaturation temperature and the correlation between these events (Wagner & Wüthrich, 1979). Our data on thioredoxin are completely in agreement with the data obtained by Kosiakoff (1982) and Wagner (1983) on other proteins where "the fluctuations that are relevant for hydrogen exchange in a β-sheet are related to the process of thermal unfolding, but different from complete denaturation". This process has sometimes been called "regional melting" (Kosiakoff, 1982) and is thought to involve the simultaneous breaking of several hydrogen bonds of a segment of secondary structure. Thus, our data suggest that such processes do occur for the β-sheet of thioredoxin, in both its oxidized and reduced state.

In conclusion, we have found that there are only minimal differences in the overall structures of the oxidized and reduced forms of thioredoxin and that the small 14-membered disulfide loop confers a stability on the overall structure of the protein that reduces the rate of the backbone hydrogen exchange and increases the stability of the protein. Structural changes that accompany the reduction of the disulfide loop could only be detected for residues in the vicinity of this redox active site.

Acknowledgments

We are indebted to Dr. Osnat Herzberg (Edmonton) for her initial help with the molecular graphics analysis.

Supplementary Material Available

Figures showing a one-dimensional comparison between the NH protons, a two-dimensional comparison of the Ile/Leu/Val region of the spectrum for the oxidized and reduced forms of thioredoxin, and the pH titration of the reduced form of the protein (3 pages). Ordering information is given on any current masthead page.

References

Anfinsen & Scheraga (1975) *Adv. Protein Chem. 29*, 205–301.
Black, S., Harte, E. M., Hudson, B., & Wartofsky, L. (1960) *J. Biol. Chem. 235*, 2910–2916.
Boyd, J., Dobson, C. M., & Redfield, C. (1985) *Eur. J. Biochem. 153*, 383–396.
Brown, S. B., Turner, R. J., Roche, R. S., & Stevenson, K. J. (1987) *Biochemistry 26*, 863–871.
Chen, G. C., & Yang, J. T. (1977) *Anal. Lett. 10*, 1195–1207.
Chen, G. C., Yang, J. T., & Chan, K. H. (1974) *Biochemistry 13*, 3050–3359.
Dalgarno, D. C., Levine, B. A., & Williams, R. J. P. (1983) *Biosci. Rep. 3*, 443–452.
Drakenberg, T., Forsén, S., Thulin, E., & Vogel, H. J. (1987) *J. Biol. Chem. 261*, 672–678.
Eklund, H., Cambillau, C., Sjöberg, D. M., Holmgren, A., Jörnvall, H., Hoog, J.-O., & Brandén, C.-I. (1984) *EMBO J. 3*, 1443–1449.
Holmgren, A. (1968) *Eur. J. Biochem. 6*, 475–484.
Holmgren, A. (1972) *J. Biol. Chem. 247*, 1992–1998.
Holmgren, A. (1979) *J. Biol. Chem. 254*, 9113–9119.
Holmgren, A. (1985) *Annu. Rev. Biochem. 54*, 237–271.
Holmgren, A., & Roberts, G. (1976) *FEBS. Lett. 71*, 261–265.
Holmgren, A., Söderberg, B.-O., Eklund, H., & Brandén, C.-I. (1975) *Proc. Natl. Acad. Sci. U.S.A. 72*, 2305–2309.
Huber, H. E., Russel, M., Model, P., & Richardson, C. C. (1986) *J. Biol. Chem. 261*, 15006–15012.

Kallis, G.-B., & Holmgren, A. (1980) *J. Biol. Chem. 255*, 10261–10265.
Kelley, R. F., Shalongo, W., Jagannadham, M. V., & Stellwagen, E. (1987) *Biochemistry 26*, 1406–1411.
Kishore, R., & Balaram, P. (1986) in *Thioredoxin and Glutaredoxin Systems: Structure and Function* (Holmgren, A., et al., Eds.) pp 57–66, Raven, New York.
Kosiakoff, A. A. (1982) *Nature (London) 296*, 713–721.
Laurent, T. C., Moore, E. C., & Reichard, P. (1964) *J. Biol. Chem. 239*, 3436–3444.
LeMaster, D. M., & Richards, F. M. (1985) *Biochemistry 24*, 7263–7268.
LeMaster, D. M., & Richards, F. M. (1988) *Biochemistry 27*, 142–150.
Lim. C.-J., Geraghty, D., & Fuchs, J. A. (1985) *J. Bacteriol. 163*, 311–316.
Lunn, C. A., Kathju, S., Wallace, B. J., Kushner, S. R., & Pigiet, V. (1984) *J. Biol. Chem. 259*, 10469–10475.
Markley, J. (1975) *Acc. Chem. Res. 8*, 70–80.
Moonen, C. T. W., Scheek, R. M., Boelens, R., & Muller, F. (1984) *Eur. J. Biochem. 141*, 323–330.
Pardi, A., Wagner, G., & Wüthrich, K. (1983) *Eur. J. Biochem. 137*, 445–454.
Perkins, S. (1982) *Biol. Magn. Reson. 4*, 193–336.
Perry, L. J., & Wetzel, R. (1986) *Biochemistry 25*, 733–739.
Pigiet, V. P., & Schuster, B. J. (1986) *Proc. Natl. Acad. Sci. U.S.A. 83*, 7643–7647.
Reutimann, H., Straub, B., Luisi, P. L., & Holmgren, A. (1981) *J. Biol. Chem. 256*, 6790–6803.
Russel, M., & Model, P. (1986) *J. Biol. Chem. 261*, 14997–15005.
Sauer, R. T., Hehir, K., Stearman, R. S., Weiss, M. A., Jeitler-Nilsson, A., Suchanek, E. G., & Pabo, C. O. (1986) *Biochemistry 25*, 5992–5998.
Siegel, J. B., Steinmetz, W. E., & Long, G. L. (1980) *Anal. Biochem. 104*, 160–167.
Stryer, L., Holmgren, A., & Reichard, P. (1967) *Biochemistry 6*, 1016–1020.
Villafranca, J. E., Howell, E. E., Voet, D. H., Strobel, M. S., Ogden, R. C., Abelson, J. N., & Kraut, J. (1983) *Science (Washington, D.C.) 222*, 782–788.
Wagner, G. (1983) *Q. Rev. Biophys. 16*, 1–57.
Wagner, G., & Wüthrich, K. (1979) *J. Mol. Biol. 130*, 31–37.
Wagner, G., Kalb, J. A., & Wüthrich, K. (1979) *Eur. J. Biochem. 95*, 249–253.
Wemmer, D., & Reid, B. R. (1985) *Annu. Rev. Phys. Chem. 36*, 105–137.
Wilson, J., Kelley, R. F., Shalongo, W., Lowly, D., & Stellwagen, E. (1986) *Biochemistry 25*, 7560–7566.
Wilson, L. G., Asahi, T., & Bandurski, R. S. (1961) *J. Biol. Chem. 236*, 1822–1829.
Wolosiuk, R. A., & Buchanan, D. B. (1977) *Nature (London) 266*, 565–567.
Woodward, C., Simon, I., & Tuchsen, E. (1982) *Mol. Cell. Biochem. 48*, 135–160.
Wüthrich, K. (1986) *NMR of Proteins and Nucleic Acids*, pp 1–293, Wiley, New York.

Orientation of Substrate and Two Conformations of Lactose Permease†

Klaus Dornmair and Fritz Jähnig*
Max-Planck-Institut für Biologie, Corrensstrasse 38, 7400 Tübingen, FRG
Received February 18, 1988

ABSTRACT: The accessibility of substrate bound to lactose permease of *Escherichia coli* was investigated by using the fluorescent substrate dansyl galactoside and a membrane-impermeable fluorescence quencher. To determine the orientation of bound substrate, both cells and inside-out vesicles were used. The substrate is oriented with the dansyl group toward the cytoplasm and the galactoside group toward the periplasm. Only half of the dansyl groups are accessible to quencher, irrespective of their orientation. This is interpreted as evidence for two different conformations of lactose permease, one with the binding site open to the cytoplasm and closed to the periplasm and vice versa for the other state.

Lactose permease (LP)[1] of *Escherichia coli* is an integral protein of the cytoplasmic membrane which uses the protonmotive force to accumulate galactosides against their concentration gradient in the cytoplasm [for reviews, see Kaback (1986) and Wright et al. (1986)]. The primary structure is known and consists of 417 amino acid residues (Büchel et al., 1980; Ehring et al., 1980). The protein was shown to be a monomer, at least in the absence of an electrochemical potential (Goldkorn et al., 1984; Dornmair et al., 1985). The secondary structure has been investigated both by circular dichroism and by Raman spectroscopy and was found to be predominantly α-helical (Foster et al., 1983; Vogel et al., 1985). Upon combination of these experimental results with structural predictions, a model for the folding of the LP within the membrane was proposed: Ten membrane-spanning α-helices form a ring whose interior is filled with relatively hydrophilic amino acid residues suited to provide the sugar binding site (Overath & Wright, 1983; Vogel et al., 1985).

†Supported by the Deutsche Forschungsgemeinschaft through Grant Ja 243/5-2.

[1] Abbreviations: LP, lactose permease; ESR, electron spin resonance; CPM vesicles, cytoplasmic membrane vesicles; ISO vesicles, inside-out vesicles; DMPC, dimyristoylphosphatidylcholine; GalSGal, β-D-galactosyl-1-thio-β-D-galactoside; DnsEtOGal, 2-(*N*-dansylamino)ethyl β-D-galactoside; NpαGal, *p*-nitrophenyl α-D-galactoside; lactose, 4-*O*-β-D-galactosyl-α-D-glucose; TEMPOamine, 2,2,6,6-tetramethyl-4-aminopiperidine 1-oxide; TMA-TEMPO, 2,2,6,6-tetramethyl-4-(trimethylammonio)piperidine 1-oxide; Tris-HCl, tris(hydroxymethyl)aminomethane hydrochloride; EDTA, ethylenediaminetetraacetic acid.

0006-2960/88/0427-5008$01.50/0